[1] E. Bright Wilson, Jr., and J. B. Howard, J. Chem. Phys. **4**, 260 (1936).

[2] J. H. Van Vleck, Phys. Rev. **33**, 467 (1929).

[3] E. C. Kemble, *Fundamental Principles of Quantum Mechanics* (Dover, New York, 1958), pp. 394–396.

[4] H. H. Nielsen, Phys. Rev. **68**, 181 (1945).

[5] R. C. Herman and W. H. Schaffer, J. Chem. Phys. **16**, 453 (1948).

[6] M. Goldsmith, G. Amat, and H. H. Nielsen, J. Chem. Phys. **24**, 1178 (1956); G. Amat, M. Goldsmith, and H. H. Nielsen, *ibid.* **27**, 845 (1957); G. Amat and H. H. Nielsen, *ibid.* **29**, 665 (1958).

[7] J. K. G. Watson, J. Chem. Phys. **46**, 1935 (1967).

[8] H. Primas, Helv. Phys. Acta **34**, 331 (1961); Rev. Mod. Phys., **35**, 710 (1963).

[9] A. M. Arthurs and P. D. Robinson, Am. J. Phys. **37**, 921 (1969); and references therein.

[10] P. O. Löwdin, J. Math. Phys. **6**, 1341 (1965).

[11] P. O. Löwdin, J. Math. Phys. **3**, 696 (1962).

[12] P. O. Löwdin, Intern. J. Quantum Chem. **2**, 867 (1968).

[13] It will be understood in this paper that if Q is a Hermitian projection operator with $\mathrm{Tr}(Q) = n$, then $\mathsf{S}(Q)$ is a n-dimensional space associated with Q.

[14] J. H. Choi, J. Math. Phys. **10**, 2142 (1969).

[15] E. P. Wigner, Math. Naturw. Anz. Ungar. Akad. Wiss. **53**, 475 (1935).

[16] For notations used here see Ref. 5.

[17] A. Messiah, *Quantum Mechanics* (North-Holland, Amsterdam, 1966), Vol. I, p. 434.

[18] P. A. M. Dirac, *The Principles of Quantum Mechanics*, 4th ed. (Oxford U. P., Cambridge, 1967), p. 139.

[19] J. O. Hirschfelder, J. Chem. Phys. **39**, 2099 (1963).

Transport of Resonance Radiation in an Infinite Cylinder

M. G. Payne and J. D. Cook

Berea College, Berea, Kentucky 40403

(Received 26 March 1970)

The Holstein-Biberman integrodifferential equation for the transport of resonance radiation has been solved for a gas contained in a long cylindrical container. The solution involves the following assumptions: (i) The excited atoms are initially distributed uniformly along the axis of the cylinder; (ii) the pressure and temperature of the gas are such that the absorption coefficient has either a pure Doppler-broadened or a pure pressure-broadened profile; (iii) the radius of the cylinder corresponds to many optical depths at the frequency corresponding to the maximum of the absorption coefficient. It is also shown that steady-state solutions corresponding to a line source along the axis of the cylinder can be calculated by the same procedure. The geometry and the initial conditions considered here are of particular interest because the situation can be simulated experimentally. Hurst and Thonnard have pointed out that an approximate line of excited atoms can be produced by sending a well-collimated pulse of protons or electrons down the axis of a long cylinder containing the gas of interest. The present paper also considers the decay of resonance radiation from a steady state built up by a line source. The latter situation is even easier to arrange experimentally. All experimental work to date has concerned itself with situations where the initial distribution of excited atoms is not known, and theory and experiment can only be compared at times which are large enough so that the system has decayed to its lowest eigenmode.

I. INTRODUCTION

The imprisonment of resonance radiation in a gas was originally treated as a diffusion problem.[1-3] However, it was later shown by Holstein[4,5] and Biberman[6] that the diffusion approximation is not valid and the problem of calculating the density of resonance atoms $N(\vec{r}, t)$ was reduced to the solution of an integrodifferential equation. This integrodifferential equation is

$$\frac{\partial N}{\partial t}(\vec{r}, t) = S(\vec{r}, t) - \gamma N(\vec{r}, t) - AN(\vec{r}, t)$$

$$+ \gamma \int G(|\vec{r} - \vec{r}\,'|) N(\vec{r}\,', t) d\vec{r}\,', \qquad (1)$$

where $S(\vec{r}, t)$ is the rate of production of excited atoms per unit volume at $\vec{r}$ by sources, A is the rate coefficient for any volume process which converts the energy associated with the excited atoms into some form other than resonance photons, γ is the reciprocal of the natural lifetime, and G is given by[4]

$$G(\rho) = -\frac{1}{4\pi\rho^2}\frac{\partial T}{\partial\rho}, \qquad (2)$$

with

$$T(\rho) = \int P(\nu)e^{-k(\nu)\rho} d\nu. \qquad (3)$$

In Eq. (3), it is assumed that

$$P(\nu) \propto k(\nu) , \qquad (4)$$

where $k(\nu)$ is the absorption coefficient and $P(\nu)\,d\nu$ is the probability of a photon being emitted by a resonance atom having a frequency between ν and $\nu + d\nu$. The whole formalism neglects any correlation between the frequency of an absorbed photon and the frequency of the photon that is subsequently emitted. Holstein[4,5] gave convincing arguments to show that Eq. (1) holds in most laboratory situations.

Up to the present time most of the solutions to Eq. (1) have used rather simple forms for $k(\nu)$ and have been for enclosures in the form of an infinite slab.[4-7] They have also assumed that the slab was excited in such a way that the density of excited atoms depends only upon the distance from the slab faces.[6,7] Since the experimentalist finds that it is quite difficult to excite a large slab in such a way that $N(\vec{r}, t)$ depends only on the distance from the slab faces, most experimental work with this geometry has concentrated on times that are so large that the system has decayed to the lowest eigenmode.[8] Holstein[4,5] showed how the large-t behavior of a gas contained in an infinite cylinder can be calculated and Walsh[9] showed how a more complicated $k(\nu)$ can be accounted for in such a calculation, but detailed calculations for cylindrical geometries do not seem to exist as they do for the slab case.[7]

Hurst and Thonnard[10] designed an experiment which should test Eq. (1) and the $k(\nu)$ used there in considerable detail. The latter experiment uses a long cylinder filled with He or Ar. The gas is excited by a beam of fast-charged particles moving down the axis of the cylinder. In this way one can produce steady states with the density of excited atoms depending only on the cylindrical coordinate ρ. One can either study the resonance radiation escaping in the steady state or pulse the beam and watch the decay of the radiation from the steady state. The purpose of the present paper is to solve Eq. (1) for cylindrical systems and densities of excited atoms which depend only on the cylindrical coordinate ρ. Equation (1) will be solved for $k(\nu)$ corresponding to both Doppler- and impact-broadened line profiles. We believe that the present theory and the Hurst-Thonnard experiment will provide the most detailed check of imprisonment theory to date.

A thorough investigation of imprisonment theory is important to the study of those collision processes which become important because of the long time that the excitation energy stays in the system. If the theory of imprisonment is very accurate, the numbers calculated from it can be used in extracting cross sections for the enhanced collision processes from the experimental data.

II. DECAY PROBLEM

In this section we assume that $S(\vec{r}) = 0$ and consider the case where at $t = 0$ there is one excited atom per unit length, all located along the axis of an infinitely long cylinder of radius R. In this case Eq. (1) becomes

$$\frac{\partial N}{\partial t}(\rho, t) = -\gamma N(\rho, t) - AN(\rho, t)$$
$$+ \gamma \int_0^R g(\rho, \rho')N(\rho', t)\rho\,d\rho' , \qquad (5)$$

where

$$g(\rho, \rho') = \int_0^{2\pi} d\phi \int_{-\infty}^{\infty} d\nu$$
$$\times G\left[(\nu^2 + \rho^2 + \rho'^2 - 2\rho\rho'\cos\phi)^{1/2}\right] . \qquad (6)$$

In calculating $N(\rho, t)$ it is convenient to divide the problem into two parts: (a) The calculation of $N(\rho, t)$ for values of t which are small enough so that a small fraction of the energy associated with the excited atoms has escaped from the system; and (b) the calculation of $N(\rho, t)$ at times which are large enough to that $N(\rho, t)$ can be accurately expanded in terms of the first six eigenfunctions of the integral operator in Eq. (5). We shall see that the two divisions of time almost overlap.

A. Solution at Early Times

We begin by noting that the presence of the boundary at $\rho = R$ does not become important until t becomes large enough so that an appreciable fraction of the possible resonance photons have crossed the boundary. Thus, at small t we can neglect the boundary and consider the problem of calculating $N(\rho, t)$ in an infinite medium.

To find $N(\rho, t)$ in an infinite medium we note that if the boundary is neglected,

$$N(\rho, t) = \int_{-\infty}^{\infty} dz\, n((z^2 + \rho^2)^{1/2}, t) , \qquad (7)$$

where $n(r, t)$ is the solution of Eq. (1) with no boundaries and the initial condition $n(r, 0) = \delta(\vec{r})$. The calculation of $n(r, t)$ has been carried out by Veklenko.[11] However, since our criteria for the validity of the derivation differ from those of Veklenko, we will repeat them:

If we let

$$g(\vec{p}, t) = \int e^{i\vec{p}\cdot\vec{r}} n(r, t)\,d\vec{r} , \qquad (8)$$

we can transform the equation for $n(r, t)$ into a solvable form. To see this, we note that

$$\frac{\partial n}{\partial t}(r, t) = -(\gamma + A)n(r, t)$$
$$+ \gamma \int G(|\vec{r} - \vec{r}'|)n(r, t)\,d\vec{r}' . \qquad (9)$$

Multiplying Eq. (9) by $e^{i\vec{p}\cdot\vec{r}}$ and integrating, we obtain

$$\frac{\partial g}{\partial t}(\vec{p},t)+(\gamma+A)g(\vec{p},t)$$

$$=\gamma\int n(r',t)\,d\vec{r}'\int e^{i\vec{p}\cdot\vec{r}}G(|\vec{r}-\vec{r}'|)\,d\vec{r}$$

$$=\gamma\int n(r',t)e^{i\vec{p}\cdot\vec{r}'}\,d\vec{r}'$$

$$\times\int e^{i\vec{p}\cdot(\vec{r}-\vec{r}')}G(|\vec{r}-\vec{r}'|)\,d\vec{r}$$

$$=\gamma g(\vec{p},t)[1-R(p)]\ ,$$

where

$$R(p)=\int(1-e^{i\vec{p}\cdot(\vec{r}-\vec{r}')})G(|\vec{r}-\vec{r}'|)\,d\vec{r}\ . \quad (10)$$

We then have

$$\frac{\partial g}{\partial t}=-Ag-\gamma R(p)g\ . \quad (11)$$

Solving Eq. (11), we get

$$g(\vec{p},t)=C(\vec{p})\exp[-At-\gamma tR(p)]\ .$$

The initial condition $n(r,0)=\delta(\vec{r})$ leads to

$$g(\vec{p},t)=\exp[-At-R(p)\gamma t]\ . \quad (12)$$

$n(r,t)$ becomes

$$n(r,t)=(2\pi)^{-3}\int e^{-i\vec{p}\cdot\vec{r}}$$

$$\times\exp[-At-R(p)\gamma t]\,dp\ . \quad (13)$$

To see what approximations might be appropriate we consider $R(p)$:

$$R(p)=2\pi\int_0^\pi \sin\phi\,d\phi\int_0^\infty u^2 G(u)$$

$$\times(1-e^{ipu\cos\phi})\,du\ .$$

The imaginary part of $R(p)$ integrates to zero if the integration over ϕ is carried out first. Thus,

$$R(p)=2\pi\int_0^\pi \sin\phi\,d\phi\int_0^\infty u^2 G(u)$$

$$\times[1-\cos(pu\cos\phi)]\,du\ . \quad (14)$$

Using the facts that $G(u)>0$, and that its volume integral over all space is unity, we see that $R(p)$ has the following properties: (a) $R(0)=0$, (b) $R(p)>0$, if $p>0$, (c) $R(p)=1$ in the limit as $p\to\infty$. If $\gamma t\gg 1$ we see from Eq. (13) that most of the contribution to $n(r,t)$ comes when $R(p)$ is very small. However, $R(p)$ is only small when p is small; and when p is small most of the contribution to $R(p)$ comes from large u. Thus, we expect that when $\gamma t\gg 1$ we can calculate $n(r,t)$ for all r while using an $R(p)$ determined from the asymptotic form of $G(u)$. The condition $\gamma t\gg 1$ is equivalent to saying that the full width at half-maximum of $n(r,t)$ is many optical depths at the center of the resonance line. In the case of pressure broadening the as-

ymptotic form of $G(u)$ can be used if $\gamma t>15$; even when γt is not large, the $R(p)$ determined from the asymptotic form of $G(u)$ yields values of $n(r,t)$ which are accurate at large r. The size of γt does not enter into Veklenko's discussion; he seems to imply that the $n(r,t)$ calculated while using the asymptotic form of $G(u)$ are only valid at large r.

In many experimental situations γt reaches a value of several hundred before the presence of the boundary becomes important. Thus, there is often a very significant period of time during which the $R(p)$ calculated from the asymptotic form of $G(u)$ can be used in calculating $n(r,t)$ at all $r<R$. We will now determine $R(p)$ in this approximation.

Holstein[5] has pointed out that when r corresponds to many optical depths at the center of the line, the transmission probability becomes

$$T(r)\approx a_m/r^m\ , \quad (15)$$

where $m=\frac{1}{2}$ for pressure broadening and $m=1$ for Doppler broadening. We rewrite Eq. (15) as

$$T(r)=T(R)(R/r)^m\ . \quad (16)$$

From Eq. (14) we obtain

$$R(p)=B_m T(R)(Rp)^m\ , \quad (17)$$

where $B_1=\frac{1}{4}\pi$ and $B_{1/2}=\frac{1}{3}(2\pi)^{1/2}$. If the angular dependence in Eq. (13) is integrated out and Eq. (17) is used, we have

$$n(r,t)=(2\pi^2 r)^{-1}e^{-At}$$

$$\times\int_0^\infty p\sin pr\exp[-B_m(Rp)^m t/T_0]\,dp\ , \quad (18)$$

with　　$T_0=[\gamma T(R)]^{-1}$. Using Eq. (18) in Eq. (7),

$$N(\rho,t)=\pi^{-2}e^{-At}\int_0^\infty p\exp[-B_m(pR)^m t/T_0]\,dp$$

$$\times\int_0^\infty \frac{\sin[p(\rho^2+z^2)^{1/2}]}{(\rho^2+z^2)^{1/2}}\,dz$$

$$=(2\pi)^{-1}e^{-At}\int_0^\infty pJ_0(\rho p)$$

$$\times\exp[-B_m(Rp)^m t/T_0]\,dp\ , \quad (19)$$

where $J_0(\rho p)$ is the Bessel function of zero order.[12] We will now work out the most important special cases.

1. Pressure Broadening

In this case we have $m=\frac{1}{2}$. Equation (19) and the substitutions $B_{1/2}=\frac{1}{3}(2\pi)^{1/2}$ and $u^2=p\rho$ yield

$$N(\rho,t)=(\pi\rho^2)^{-1}e^{-At}H(y)\ , \quad (20)$$

where

$$y=\frac{1}{3}(2\pi)^{1/2}(R/\rho)^{1/2}(t/T_0)$$

and   (21)

$$H(y) = \int_0^\infty u^3 J_0(u^2) e^{-uy} du .$$

Several of the more important properties of $H(y)$ are derived in the Appendix. Further, $H(y)$ is tabulated in Table I.

In dealing with our finite geometry it is convenient to let $s = \rho/R$ and to introduce a new function $M(s, t)$ with the property $2\pi M(s, t)sds = 2\pi N(\rho, t)\rho d\rho$. Thus, $M(s, t) = R^2 N(\rho, t)$, and Eq. (20) becomes

$$M(s, t) = (\pi s^2)^{-1} e^{-At} H(y) .$$ (22)

Figures 1 and 2 compare $M(s, t)$, calculated from Eq. (22), with a more exactly computed $M(s, t)$ at the times $t = T_0$ (Fig. 1) and $t = 2T_0$ (Fig. 2). The calculation of the more exact $M(s, t)$ will be discussed in Sec. II B. At $t = T_0$, 39% of the original excited atoms are still in the system (assuming $A = 0$) and Eq. (22) remains accurate except at points which are very near the wall of the container. At $t = 2T_0$ only 14% of the original excited atoms remain and Eq. (22) is beginning to become rather inaccurate over the outer half of the cylinder.

The experiment is often interested in the fraction of the excited atoms that remain in the system after a time t. We designate this fraction by $N_T(t)$ and note that

$$N_T(t) = 2\pi \int_0^R N(\rho, t) \rho d\rho = 2\pi \int_0^1 M(s, t)s ds .$$ (23)

When t is small enough so that Eq. (22) is valid, we find

$$N_T(t)e^{At} = 2 \int_0^1 H(y) ds/s;$$

TABLE I. Tabulation of the function $H(X)$.

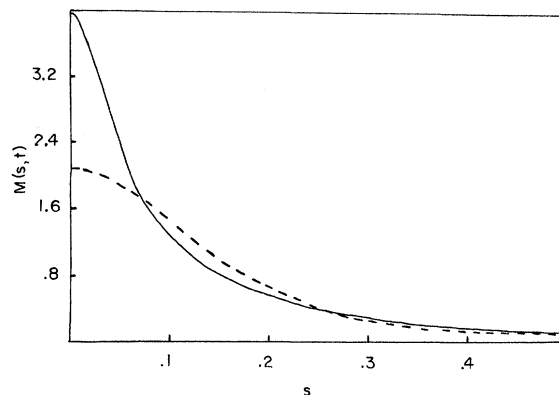| X	H(X)	X	H(X)
0.0	0.0000	2.0	0.0610
0.1	0.0237	2.2	0.0538
0.2	0.0430	2.4	0.0471
0.3	0.0583	2.6	0.0410
0.4	0.0702	2.8	0.0357
0.5	0.0791	3.0	0.0309
0.6	0.0855	3.4	0.0232
0.7	0.0896	3.8	0.0174
0.8	0.0920	4.2	0.0131
0.9	0.0929	4.6	0.0099
1.0	0.0925	5.0	0.0076
1.1	0.0912	5.4	0.0059
1.2	0.0891	5.8	0.0046
1.4	0.0832	6.2	0.0036
1.6	0.0761	6.6	0.0029
1.8	0.0685		

FIG. 1. Pressure-broadened $M(s, t)$ at time $t = T_0$. Solid curve, calculated while neglecting the effect of the boundary. Dashed curve, calculated from the first six terms in the eigenfunction expansion. The curve for the 20-term eigenfunction expansion lies so close to that calculated while neglecting the presence of the boundary, that clutter would result if it were shown.

now, we have

$$y = \tfrac{1}{3}(2\pi)^{1/2}(t/T_0)s^{-1/2},$$

so that

$$N_T(t) e^{At} = 4 \int_{1/3(2\pi)^{1/2}t/T_0}^{\infty} H(y) \, dy/y$$

$$= 1 - 4 \int_0^{1/3(2\pi)^{1/2}t/T_0} H(y) \, dy/y .$$ (24)
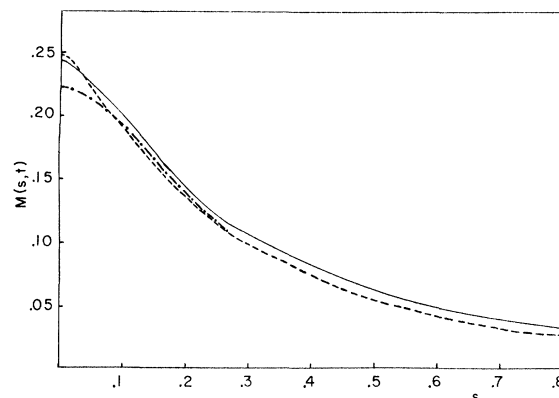
Let

$$L(x) = 1 - 4 \int_0^x H(y) \, dy/y .$$

FIG. 2. Pressure-broadened $M(s, t)$ at time $t = 2T_0$. Solid curves calculated while neglecting the presence of the boundary. Dashed curve calculated from the first twenty terms of the eigenfunction expansion. Dot-dashed curve, calculated from the first six terms in the eigenfunction expansion. When $s > 0.3$, the curves for the 20- and 6-term eigenfunction expansions coincide.

The function $L(x)$ is tabulated in Table II. Equation (24) can now be written as

$$N_T(t)\, e^{At} = L(\tfrac{1}{3}(2\pi)^{1/2} t/T_0) \ . \tag{25}$$

Figure 3 compares $N_T(t)\, e^{At}$, calculated from Eq. (25), with a more exact calculation to be discussed in Sec. II B. In the pressure-broadening region, Eqs. (22) and (25) are useful for $t < 1.5T_0$.

2. Doppler Broadening

In this case we have $m = 1$. Equation (19) and the substitutions $B_1 = \tfrac{1}{4}\pi$ and $u = \rho p$ yield[12]

$$M(s,t) = \frac{t}{8T_0}\left[s^2 + \left(\frac{\pi t}{4T_0}\right)^2\right]^{-3/2} . \tag{26}$$

Figures 4 and 5 compare $M(s,t)$, calculated from Eq. (26), with a more accurately computed $M(s,t)$ at the time $t = 0.4T_0$ (Fig. 4) and $t = 0.6T_0$ (Fig. 5). At $t = 0.4T_0$ about 67% of the excited atoms (assuming $A = 0$) remain inside the cylinder and Eq. (26) is still fairly accurate except in the region near the walls of the container. At $t = 0.6T_0$ Eq. (26) is quite inaccurate over the outer half of the volume of the cylinder. In the $t = 0.6T_0$ case about 52% of the excited atoms remain in the system.

From Eq. (26) we find

$$e^{At}N_T(t) = 1 - (\pi t/4T_0)[1 + (\pi t/4T_0)^2]^{-1/2} \ . \tag{27}$$

Both Eqs. (26) and (27) become inaccurate for $t > 0.4T_0$. However, at larger times the method to be discussed in Sec. II B becomes quite easy to use.

In order to calculate T_0 we use $T_0 = [\gamma T(R)]^{-1}$ along with Holstein's[5] explicit formulas for the asymptotic form of the transmission probability. When $m = 1$ we have

$$T_0 = \tau(k_0 R)[\pi \ln(k_0 R)]^{1/2} \ , \tag{28a}$$

where τ is the natural lifetime and k_0 is the absorption coefficient evaluated at the center of the resonance line. When $m = \tfrac{1}{2}$ we have

$$T_0 = \tau(\pi k_p R)^{1/2} \ , \tag{28b}$$

TABLE II. Tabulation of the function $L(X)$.

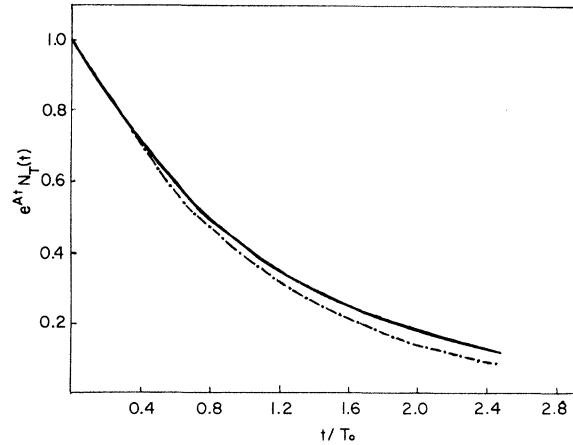| X	L(X)	X	L(X)
0.0	1.000	1.1	0.306
0.1	0.900	1.2	0.274
0.2	0.810	1.3	0.246
0.3	0.728	1.4	0.221
0.4	0.654	1.5	0.199
0.5	0.587	1.6	0.179
0.6	0.527	1.7	0.161
0.7	0.473	1.8	0.145
0.8	0.424	1.9	0.130
0.9	0.380	2.0	0.118
1.0	0.341		

FIG. 3. Pressure-broadened $e^{At}N_T(t)$ as a function of time. Solid curve, calculated while neglecting the effect of the boundary. Dot-dashed curve, calculated from the 20-term eigenfunction expansion.

where k_p is the maximum value of the absorption coefficient when pressure broadening dominates. Holstein[5] also discusses the calculation of k_0 and k_p from more fundamental quantities. As in Holstein's papers, we have assumed that both $k_p R$ and $k_0 R$ are very large numbers.

It should be mentioned that Walsh's formula for $T(R)$ provides a convenient way of determining if either Doppler or pressure broadening is dominant. If either dominates the other, Walsh's formula
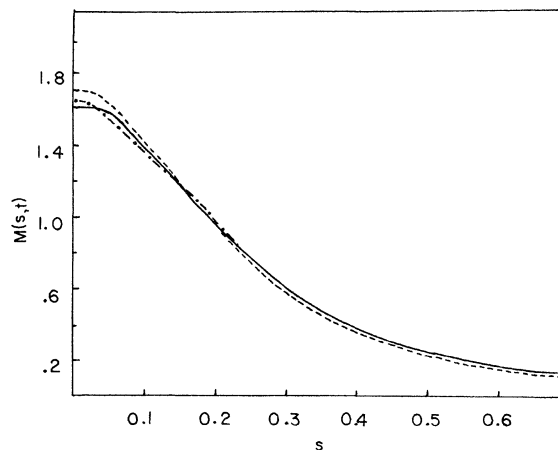

FIG. 4. Doppler-broadened $M(s, t)$ at time $t = 0.4T_0$. Solid curve calculated while neglecting the effect of the boundary. Dashed curve, calculated from the 20-term eigenfunction expansion. Dot-dashed curve, calculated from the first six terms of the eigenfunction expansion. When $s > 0.3$ the curves for the 6- and 20-term eigenfunction expansions almost coincide.

FIG. 5. Doppler-broadened $M(s,t)$ at time $t = 0.6T_0$. Solid curve, calculated while neglecting the presence of the boundary. Dashed curve, calculated from the first twenty terms of the eigenfunction expansion. Dot-dashed curve, calculated from the first six terms of the eigenfunction expansion. When $s > 0.2$ the curves for the 6- and 20-term eigenfunction expansions almost coincide.
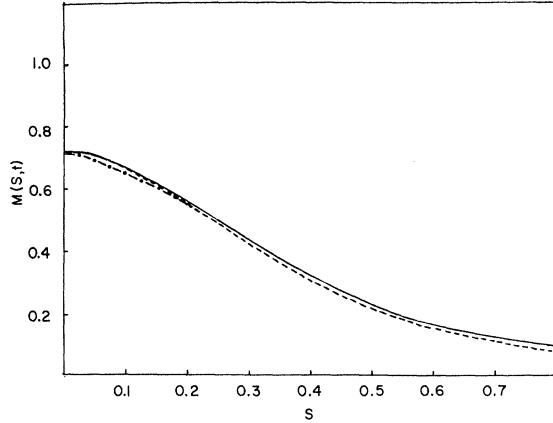
can be approximated accurately by one of the $T(R)$'s for the special cases of Doppler and pressure broadening.

B. Solution at Intermediate and Large Times

In this region of time we will use the Hilbert-Schmidt method[13] in order to solve Eq. (5). In this method we introduce eigenfunctions $\phi_k(\rho)$ and eigenvalues λ_k defined by the equation

$$(1 - \lambda_k)\,\phi_k(\rho) = \int_0^R \phi_k(\rho')g(\rho,\,\rho')\,\rho'\,d\rho' \ . \quad (29)$$

It is convenient to let $\psi_k(\rho) = \rho^{1/2}\phi_k(\rho)$ and $g_0(\rho,\,\rho') = (\rho\rho')^{1/2}g(\rho,\,\rho')$. Equation (29) then becomes

$$(1 - \lambda_k)\,\psi_k(\rho) = \int_0^R \psi_k(\rho')g_0(\rho,\,\rho')\,d\rho' \ . \quad (30)$$

From Eq. (6) we see that $g(\rho,\,\rho') = g(\rho',\,\rho)$, so that $g_0(\rho,\,\rho') = g_0(\rho',\,\rho)$. In Chap. 3 of Courant and Hilbert[13] it is shown that the λ_k are denumerable and real. It is also shown that the $\psi_k(\rho)$ are orthogonal and can be chosen to be real. Thus, they can be normalized so that

$$\int_0^R \psi_k(\rho)\psi_i(\rho)\,d\rho = \delta_{k,i} \ . \quad (31)$$

In our special case we can use Eq. (29), the properties of the $\psi_k(\rho)$, and the fact that $g(\rho,\rho')$ is a probability density to show that the λ_k are positive and less than unity. We will henceforth assume that the λ_k have been arranged in an ascending sequence of positive numbers.

From Eq. (31) and the definition of the $\psi_k(\rho)$ we

see that the $\phi_k(\rho)$ can be chosen real and that they are orthogonal with weight function ρ. The $\phi_k(\rho)$ can be normalized so that

$$\int_0^R \phi_k(\rho)\phi_i(\rho)\,\rho\,d\rho = \delta_{k,i} \ . \quad (32)$$

We expand $N(\rho,t)$ as

$$N(\rho,t) = e^{-At}\sum_{k=1}^{\infty} a_k(t)\phi_k(\rho) \ . \quad (33)$$

Substituting into Eq. (5) and using Eqs. (29) and (32), we find

$$a_k(t) = d_k e^{-\gamma\lambda_k t} \ ,$$

where the d_k are constants. Thus,

$$N(\rho,t) = e^{-At}\sum_{k=1}^{\infty} d_k e^{-\gamma\lambda_k t}\phi_k(\rho) \ . \quad (34)$$

Evaluating the last equation at $t = 0$ and using Eq. (32) we find

$$d_k = \int_0^R N(\rho,0)\phi_k(\rho)\,\rho\,d\rho \ . \quad (35)$$

In the special case under consideration $N(\rho,0) = \delta(\rho)/(2\pi\rho)$, so that

$$N(\rho,t) = e^{-At}(2\pi)^{-1}\sum_{k=1}^{\infty} e^{-\gamma\lambda_k t}\phi_k(0)\phi_k(\rho) \ . \quad (36)$$

Holstein[4,5] used a similar approach, but he deals only with times that are so large that the $k = 1$ term is dominant. Van Trigt[7] calculated accurate eigenfunctions and eigenvalues for slab geometry.

We now show how eigenfunctions and eigenvalues can be calculated for the cylinder in the special cases of pure Doppler broadening and pure pressure broadening. We will assume, as before, that k_0R and k_pR are very large (say >400). Once the eigenfunctions and eigenvalues are determined we will be able to deal with either the decay or the steady-state problems.

For either Doppler or pressure broadening, we have

$$G(u) = mT(R)R^m/(4\pi u^{m+3}) \ , \quad (37)$$

if $k_0u \gg 1$ (or $k_pu \gg 1$). Equation (37) involves the same approximation as Eq. (16). $G(u)$ also has the property

$$\int_{\text{all space}} G(|\vec{r} - \vec{r}\,'|)\,dV' = 1 \ . \quad (38)$$

From Eq. (38), we have

$$\int_0^{\infty} g(\rho,\,\rho')\,\rho'\,d\rho' = 1 \ . \quad (39)$$

To find λ_k and $\phi_k(\rho)$ we divide the cross section of the cylinder into N concentric rings of thickness R/N. We note that in many experiments N could

be quite large (say 25) and yet R/N could still be such that $k_0 R/(2N) \gg 1$. If N is large we expect that the first several $\phi_k(\rho)$ will be almost constant over any given ring. Therefore,

$$\int_0^R \phi_k(\rho')g(\rho, \rho')\rho'\, d\rho'$$

$$= \sum_{i=1}^N \int_{R(i-1)/N}^{Ri/N} g(\rho, \rho')\phi_k(\rho')\rho'\, d\rho'$$

$$\approx \sum_{i=1}^N \phi_k(\rho_i)\int_{(R/N)(i-1)}^{(R/N)i} g(\rho, \rho')\rho'\, d\rho', \quad (40)$$

where $\rho_i = (R/N)(i-\frac{1}{2})$ is the value of ρ at the center of the ith ring. The approximation made in Eq. (40) will obviously be poor unless $N \gg k$. However, with $N = 25$ we might expect that the approximation will be quite good for $k \leq 6$. If we now evaluate both sides of Eq. (29) at ρ_n and use Eq. (40), we get

$$(1 - \lambda_k)\phi_k(\rho_n) = \sum_{i=1}^N \phi_k(\rho_i)$$

$$\times \int_{(R/N)(i-1)}^{(R/N)i} g(\rho_n, \rho')\rho'\, d\rho'. \quad (41)$$

Equation (41) is a matrix eigenvalue problem with the components of the eigenvectors being the values of the $\phi_k(\rho)$ at the points $\rho_1, \rho_2, \rho_3, \cdots, \rho_N$. We will now show how the matrix of coefficients in Eq. (41) can be calculated.

We define $A(n, i)$ as

$$A(n, i) = \int_{(R/N)(i-1)}^{(R/N)i} g(\rho_n, \rho')\rho'\, d\rho'. \quad (42)$$

Since $(k_0 R)/(2N)$ is large by assumption we can calculate $A(n, i)$ for $n \neq i$ while using an approximate $g(\rho, \rho')$ derived from Eq. (37):

$$g(\rho, \rho') = mT(R)R^m (4\pi)^{-1} \int_0^{2\pi} d\phi$$

$$\times \int_{-\infty}^{\infty} [q^2 + (z - z')^2]^{-(m+3)/2}\, dz'$$

$$= mC_m T(R)R^m$$

$$\times \int_0^{2\pi} (\rho^2 + \rho'^2 - 2\rho\rho' \cos\phi)^{-(m+2)/2}\, d\phi, \quad (43)$$

where

$$C_m = 2^{-(m+3)} m(m+1)! \left\{ [\tfrac{1}{2}(m+1)]! \right\}^{-2}, \quad (44)$$

and

$$q^2 = \rho^2 + \rho'^2 - 2\rho\rho' \cos\phi.$$

Defining

$$s_v(x) = 2 \int_0^\pi (1 + x^2 - 2x \cos\phi)^{-v}\, d\phi, \quad (45)$$

we find that for $n \neq i$,

$$A(n, i) = C_m T(R)[R/(n-\tfrac{1}{2})]^m \int_{(i-1)/(n-1/2)}^{i/(n-1/2)} S_v(x)x\, dx, \quad (46)$$

with $v = \frac{1}{2}(m+2)$. When $n = i$ we can use Eq. (39) to show that

$$A(n, n) = 1 - \int_{(R/N)n}^{\infty} g(\rho_n, \rho')\rho'\, d\rho'$$

$$- \int_0^{(R/N)(n-1)} g(\rho_n, \rho')\rho'\, d\rho'$$

$$= 1 - C_m T(R)[N/(n-\tfrac{1}{2})]^m$$

$$\times \left[\int_0^{(n-1)/(n-1/2)} S_v(x)x\, dx \right.$$

$$\left. + \int_{n/(n-1/2)}^{\infty} S_v(x)x\, dx \right]. \quad (47)$$

The reader can easily see the importance of $S_v(x)$ in the present problem. One very useful property of $S_v(x)$ is obvious from Eq. (45):

$$S_v(1/x) = x^{2v} S_v(x). \quad (48)$$

We also note that $S_v(-x) = S_v(x)$. It is also known[12] that $S_v(x)$ is related to the Gauss hypergeometric function by

$$S_v(x) = 2\pi F(v, v; 1; x^2). \quad (49)$$

Using the hypergeometric series we have[12]

$$S_v(x) = 2\pi \sum_{k=0}^{\infty} [(v)_k]^2 x^{2k}/(k!)^2, \quad (50)$$

where $(v)_k = v(v+1)(v+2)\cdots(v+k-1)$ for $k \geq 1$ and $(v)_0 = 1$. Equation (50) can be used to calculate $S_v(x)$ for the values of v that interest us here and for $0 \leq x < 1$. Equation (50) can be combined with Eq. (48) in order to calculate $S_v(x)$ for $x > 1$.

When x is close to unity most of the contribution to the integral in Eq. (45) comes from the region near $\phi = 0$. Over this region where the contribution occurs we can use $1 + x^2 - 2x \cos\phi \approx (1-x)^2 + x\phi^2$. Extending the integral over ϕ to infinity and integrating, we obtain the following approximation for small values of $|1 - x|$ and $v > \frac{1}{2}$:

$$S_v(x) \approx \pi 2^{2(1-v)} x^{-1/2} \Gamma(2v-1)[\Gamma(v)]^{-2}/|1-x|^{(2v-1)}. \quad (51)$$

Equation (51) is very useful in the region $0.7 \leq x < 1.0$. In the latter region many terms must be retained in order to calculate $S_v(x)$ accurately from Eq. (50).

It is convenient to define the matrix

$$B(n, i) = -[N/(n-\tfrac{1}{2})]^m \int_{(i-1)/(n-1/2)}^{i(n-1/2)^{-1}} S_v(x)x^{1/2}\, dx, \quad (52)$$

when $n \neq i$ and

$$B(n, n) = [N/(n - \tfrac{1}{2})]^m \left[\int_0^{(n-1)/(n-1/2)} S_\nu(x) x \, dx \right.$$

$$\left. + \int_0^{(n-1/2)/n} S_\nu(x) x^{(m-1)} \, dx \right] \quad (53)$$

It is found that if both i and n are greater than 5 we have

$$A(n, i) \approx -C_m T(R)[(i - \tfrac{1}{2})/(n - \tfrac{1}{2})]^{1/2} B(n, i) , \quad (54)$$

for $n \neq i$ and

$$A(n, n) = 1 - C_m T(R) B(n, n) . \quad (55)$$

When Eqs. (54) and (55) are used in (41) we find

$$\beta_k \Psi_k(\rho_n) = \sum_{i=1}^{N} \Psi_k(\rho_i) B(n, i) , \quad (56)$$

with

$$\lambda_k = C_m T(R) \beta_k = T(R) \beta_k' , \quad (57)$$

and

$$\Psi_k(\rho_n) = [(n - \tfrac{1}{2})/N]^{1/2} \phi_k(\rho_n) . \quad (58)$$

The approximation involved in Eq. (54) becomes more and more accurate as n and i increase and is not completely out of the ball park when $n = 1$ and $i = 2$. The biggest stimulus for introducing the $B(n, i)$ is that they can be shown to satisfy $B(n, i) \approx B(i, n)$ if both n and i are greater than 5. The symmetry relation is not seriously in error for smaller n and i. In the limit of large N the $B(n, i)$ can be treated as symmetric and the error involved in Eq. (54) is insignificant. The IBM scientific subroutine EIGEN has been used to find the β_k and $\Psi_k(\rho_n)$ for $N = 5$, 10, 20, and 25. In each case $B(n, i)$ was computed for $i \leq n$ and the $\beta(n, i)$ for $n > i$ were determined by the approximation $B(n, i) = B(i, n)$. The use of the symmetry condition was required because EIGEN requires that the matrix under consideration be symmetric.

Table III shows how the first five eigenvalues change with N for the case of pure pressure broadening. Table IV is the corresponding material for pure Doppler broadening. Table V and VI give $\Phi_k(s) = \phi_k(\rho)/R$ for $k = 1, 2, \ldots, 6$, and Tables VII

TABLE III. Convergence of the first five eigenvalues to a limit as N is increased. These eigenvalues are for pure pressure broadening.

N	β_1'	β_2'	β_3'	β_4'	β_5'
5	1.111	1.809	2.253	2.559	2.746
10	1.121	1.846	2.356	2.755	3.083
15	1.122	1.855	2.371	2.789	3.147
20	1.123	1.856	2.374	2.798	3.163
25	1.123	1.856	2.375	2.800	3.168

TABLE IV. Convergence of the first five eigenvalues to a limit as N is increased. These eigenvalues correspond to pure Doppler broadening.

N	β_1'	β_2'	β_3'	β_4'	β_5'
5	1.481	3.561	5.309	6.643	7.47
10	1.540	3.850	6.050	8.102	9.96
15	1.560	3.929	6.244	8.486	10.63
20	1.572	3.963	6.328	8.646	10.91
25	1.575	3.983	6.372	8.731	11.05

and VIII give the corresponding b_k and eigenvalues. The latter tables were calculated with $N = 25$. Table V is for pressure broadening and Table VI is for Doppler broadening.

It should be noted that the $\Phi_k(s)$ tablulated in Tables V and VI are normalized so that

$$\int_0^1 \Phi_k(s) \Phi_i(s) s \, ds = \delta_{k,i} . \quad (59)$$

Tables VII and VIII give values for the first six b_k, where

$$b_k = \int_0^1 \Phi_k(s) s \, ds . \quad (60)$$

From Eq. (36) and the definition of $M(s, t)$ we see that

$$M(s, t) = e^{-At} (2\pi)^{-1} \sum_{k=1}^{\infty} e^{-\beta_k' t/T_0} \Phi_k(0) \Phi_k(s) , \quad (61)$$

where $\beta_k' = c_m \beta_k$. Correspondingly,

$$N_T(t) e^{At} = \sum_{k=1}^{\infty} e^{-\beta_k' t/T_0} b_k \Phi_k(0) . \quad (62)$$

The more accurate curves in Figs. 1–5 were calculated from Eqs. (61) and (62) while using the approximate $\Phi_k(s)$ and β_k' determined with $N = 20$. When all 20 terms are retained in the eigenfunction expansion, we obtain much better results than are

TABLE V. Eigenfunctions for pure pressure broadening.

s	$\Phi_1(s)$	$\Phi_2(s)$	$\Phi_3(s)$	$\Phi_4(s)$	$\Phi_5(s)$	$\Phi_6(s)$
0.00	2.21	−3.97	5.12	6.19	7.10	7.90
0.02	2.21	−3.93	5.02	6.01	6.84	7.59
0.06	2.20	−3.79	4.63	5.21	5.43	5.39
0.14	2.18	−3.48	3.52	2.83	1.4-	−1.49
0.22	2.14	−2.89	1.80	−0.10	−2.01	−2.94
0.30	2.06	−2.15	0.01	−2.04	−2.44	−0.78
0.38	1.96	−1.25	−1.37	−2.18	−0.28	2.01
0.46	1.83	−0.38	−2.01	−0.82	1.75	1.31
0.54	1.69	0.39	−1.82	0.90	1.57	−1.24
0.62	1.52	0.99	−0.99	1.77	−0.31	−1.53
0.70	1.33	1.36	0.09	1.32	−1.64	0.59
0.78	1.13	1.48	1.00	0.01	−1.05	1.59
0.86	0.90	1.33	1.40	−1.14	0.61	0.06
0.94	0.62	0.94	1.16	−1.29	1.35	−1.34

TABLE VI. Eigenfunctions for pure Doppler
broadening.

s	$\Phi_1(s)$	$\Phi_2(s)$	$\Phi_3(s)$	$\Phi_4(s)$	$\Phi_5(s)$	$\Phi_6(s)$
0.00	2.36	−4.00	−5.13	−6.14	7.01	−7.88
0.02	2.36	−3.96	−5.04	−6.00	6.80	−7.51
0.06	2.33	−3.83	−4.68	−5.25	5.48	−5.43
0.14	2.31	−3.47	−3.49	−2.77	1.41	0.25
0.22	2.25	−2.85	−1.73	0.19	−2.07	2.96
0.30	2.16	−2.02	0.10	2.11	−2.40	0.66
0.38	2.03	−1.11	1.47	2.15	−0.14	−2.07
0.46	1.88	−0.20	2.03	0.69	1.83	−1.18
0.54	1.70	0.58	1.74	−1.02	1.48	1.35
0.62	1.50	1.15	0.83	−1.78	−0.46	1.44
0.70	1.28	1.47	−0.29	−1.19	−1.66	−0.73
0.78	1.04	1.52	−1.15	0.18	−0.89	−1.53
0.86	0.78	1.29	−1.45	1.25	0.77	1.18
0.94	0.48	0.83	−1.09	1.26	1.36	1.38

obtained by truncating after six terms. This is
easily seen from the good agreement obtained in
Figs. 1, 3, and 4 with the $M(s, t)$ calculated while
neglecting the presence of the cylinder walls. At
the fairly early times under consideration the
cylinder walls are unimportant except in the re-
gion very near $s = 1$. At the later times shown in
Figs. 2 and 5 the convergence of the eigenfunction
expansion has become rapid enough so that trunca-
tion after six terms gives results which are fairly
accurate.

A few words about the accuracy of the eigen-
values and the eigenfunctions given in Tables
V–VIII is appropriate here. Because of the rapid
convergence with increasing N, we believe that
the first five eigenvalues for the pressure broad-
ened case are all accurate to 1%. In the Doppler-
broadened case 1% accuracy is probably obtained
for β_1', β_2', and β_3', but β_6' may be in error by as
much as 5%. The reader will note that Holstein's[5]
best estimates of β_1' (in his notation g_{01}) are rather
close to our values. He obtains $\beta_1' \leq 1.6$ for the
Doppler-broadened case. There seems to have
been a misprint in his value of β_1' for the pressure-
broadened case. His table gives $\beta_1' \leq 1.115$, but
a recalculation yields $\beta_1' \leq 1.125$. The eigenfunc-
tions given in Tables V and VI are probably in
error by a few percent, with the accuracy being

TABLE VII. Values of β_n' and b_n for pure pressure
broadening.

n	β_n'	b_n
1	1.123	0.658
2	1.856	0.196
3	2.37	0.113
4	2.80	−0.077
5	3.17	0.058
6	3.50	−0.046

TABLE VIII. Values of β_n' and b_n for pure Doppler
broadening.

n	β_n'	b_n
1	1.575	0.640
2	3.98	0.220
3	6.37	−0.132
4	8.73	0.092
5	11.1	0.071
6	13.3	0.056

best for $\Phi_1(s)$ and poorest for $\Phi_6(s)$.

It is remarkable that in the limit of large $k_0 R$
(or $k_p R$), the calculation of $M(s, t)$ can be carried
out for all but the earliest times without any in-
clusion of the detailed behavior of $G(|\vec{r} - \vec{r}\,'|)$ at
small distances. This lack of sensitivity to the
behavior of G at small distances together with its
rather simple behavior at larger distances has
made possible the calculation of a set of eigen-
functions and eigenvalues that can be used for
cylinders of all radii and for all gas pressures
such that imprisonment is great and either pres-
sure or Doppler broadening is dominant. The in-
sensitivity to the detailed behavior of $G(|\vec{r} - \vec{r}\,'|)$
at small distances has a physical interpretation:
When $k_0 R$ (or $k_p R$) is very large the probability of
any significant penetration of a photon before ab-
sorption depends on the asymptotic form of G, but
significant penetrations occur frequently enough
(because of the slow rate of decrease of $G(r)$ with
r at large $k_0 r$) so that all significant spreading of
$M(s, t)$ occurs because of these large penetrations.

III. STEADY-STATE SOLUTIONS

We assume that the source function is a function
of ρ only. In the steady state Eq. (1) becomes

$$(\gamma + A)N(\rho) = S(\rho) + \gamma \int_0^R g(\rho, \rho\,')N(\rho\,')\rho\,' \, d\rho\,' . \quad (63)$$

We write

$$N(\rho) = \sum_{k=1}^{\infty} F_k \phi_k(\rho) . \quad (64)$$

Substituting into Eq. (63) and using Eq. (32) we
have

$$F_k = [T_0/(AT_0 + \beta_k')] \int_0^R S(\rho)\phi_k(\rho)\rho \, d\rho . \quad (65)$$

We consider the special case of a line source
producing one resonance atom per unit length per
unit time. In this case $S(\rho) = \delta(\rho)/2\pi\rho$ and

$$F_k = [T_0/(AT_0 + \beta_k')](2\pi)^{-1} \phi_k(0) . \quad (66)$$

Using Eq. (66) we have

$$N(\rho) = \frac{T_0}{2\pi} \sum_{k=1}^{\infty} \frac{\phi_k(0)\phi_k(\rho)}{AT_0 + \beta_k'} \ . \tag{67}$$

Comparing Eqs. (67) and (36) we see that

$$N(\rho) = \int_0^{\infty} N(\rho, t)dt \ . \tag{68}$$

When AT_0 is less than unity and ρ is not too small we can calculate $N(\rho)$ fairly accurately with the first six terms of Eq. (67). However, when AT_0 is considerably larger than unity $N(\rho)$ is sharply peaked near $\rho = 0$ and a large fraction of the resonance atoms lie near this region. This corresponds to the situation where the resonance atoms lose their energy by the rate process before they wander very far from $\rho = 0$. In the latter situation we use Eq. (68) and break $N(\rho)$ up into two parts. Thus, we have

$$N(\rho) \approx N_1(\rho) + N_2(\rho) \ , \tag{69}$$

with

$$N_1(\rho) = \int_0^{t_1} N(\rho, t)dt \ , \tag{70}$$

and

$$N_2(\rho) = (2\pi)^{-1} T_0 \sum_{k=1}^{6} \exp\left[-(AT_0 + \beta_k')t_1/T_0 \right]$$
$$\times \phi_k(0)\phi_k(\rho)/(AT_0 + \beta_k') \ . \tag{71}$$

In Eqs. (70) and (71) t_1 is the largest time at which Eqs. (20) or (26) remain valid. We use Eqs. (20) or (26) in evaluating $N_1(\rho)$. In the case of Doppler broadening we can use $t_1 = 0.4T_0$, while in the case of pressure broadening, $t_1 = 1.5T_0$ can be used. In this way accurate steady states can be calculated for all A and ρ with only six eigenfunctions. Unfortunately, a minor numerical calculation is required in calculating $N_1(\rho)$ for any particular A and ρ.

The experimentalist may be interested in building up a steady state and then observing the decay after the source is switched off. If the source was a line source which produced Σ_0 excited atoms per unit time per unit length we find that $N_s(t)$, the number of excited atoms remaining in the system at a time t after the source was switched off, is given by

$$N_s(t) = \Sigma_0 T_0 e^{-At} \sum_{k=1}^{\infty} \exp(-\beta_k't/T_0) \frac{b_k\phi_k(0)}{AT_0 + \beta_k'} \ . \tag{72}$$

If AT_0 is smaller than unity, Eq. (72) can be truncated after six terms. However, when AT_0 is larger than unity one needs more than six terms at small t. If AT_0 is much greater than unity, essentially every excited atom loses its energy through the volume process, and in the steady state

$N_s(0)A = \Sigma_0$. Thus, at $t = 0$ we have $N_s(0) = \Sigma_0/A$ and the excited atoms are all very near $\rho = 0$. Thus, the decay will be just like the case where there was a line of excited atoms at $t = 0$. We have

$$N_s(t) \approx (\Sigma_0/A)N_T(t), \quad AT_0 \gg 1, \tag{73}$$

where the calculation of $N_T(t)$ has been discussed in Sec. II.

ACKNOWLEDGMENTS

APPENDIX

The function $H(y)$ is defined by Eq. (21). The properties of this function do not seem to be well known. For this reason we will work out some of the simpler results that can be shown to hold.

We first note that if y is very large almost all of the contribution to the integral in Eq. (21) comes from quite small values of U, where $J_0(U^2)$ can be accurately represented by the first few terms of a Taylor series. Thus, we arrive at the asymptotic series

$$H(y) = \frac{6}{y^4}\left[1 - \frac{210}{y^4} + \cdots \right] \ , \tag{A1}$$

which is quite accurate for $y > 6$.

To arrive at an alternative integral representation for $H(y)$, we note that

$$H(y) = \mathrm{Re} \int_0^{\infty} U^3 H_0^{(1)}(U^2) e^{-yU}dU \ , \tag{A2}$$

where $H_0^{(1)}(U^2)$ is the zeroth-order Hankel function of the first kind. If U is thought of as a complex variable it can be shown that the integral from 0 to ∞ along the real axis is equal to the integral from the origin to ∞ along a line inclined at 45° above the real axis. Thus, Eq. (A2) becomes

$$H(y) = \frac{2}{\pi} \int_0^{\infty} r^3 e^{-\sqrt{2}yr} K_0(r^2) \sin \frac{yr}{\sqrt{2}} \, dr \ , \tag{A3}$$

where $K_0(r^2)$ is a zeroth-order Bessel function of imaginary argument and we have used[12]

$$K_0(r^2) = \tfrac{1}{2} i\pi H_0^{(1)}(ir^2) \ .$$

Equation (A3) is much easier to work with than Eq. (21), because the integrand decreases rapidly with increasing r for all $y > 0$.

A Taylor series for $H(y)$ can be obtained by writing

$$H(y) = \mathrm{Im} \frac{2}{\pi} \int_0^{\infty} r^3 K_0(r^2) \exp(e^{i3\pi/4}yr) dr \ ,$$

and expanding the exponential function in a Taylor series. Noting that[12]

$$\int_0^\infty t^\mu K_0(t)\, dt = 2^{\mu-1} \left[\Gamma\!\left(\frac{u+1}{2}\right) \right]^2 ,$$

we obtain

$$H(x) = \pi^{-1} \sum_{n=0}^{\infty} \sin(\tfrac{3}{4} n\pi)[\Gamma(1+\tfrac{1}{4}n)]^2 (2x)^n / n! . \quad \text{(A4)}$$

The series converges for all x.

[1]K. T. Compton, Phys. Rev. 20, 283 (1922).

[2]F. A. Horton and A. C. Davies, Phil. Mag. 44, 1140 (1922).

[3]E. A. Milne, J. London Math. Soc. 1, 40 (1926).

[4]T. Holstein, Phys. Rev. 72, 1212 (1947).

[5]T. Holstein, Phys. Rev. 83, 1159 (1951).

[6]L. M. Biberman, Zh. Eksperim. i Teor. Fiz. 17, 416 (1947) [Soviet Phys. JETP 19, 584 (1949)].

[7]C. Van Trigt, Phys. Rev. 181, A97 (1969).

[8]M. W. Zemansky, Phys. Rev. 29, 513 (1927).

[9]P. J. Walsh, Phys. Rev. 116, 511 (1959).

[10]G. S. Hurst, University of Kentucky Progress Report (unpublished).

[11]B. A. Veklenko, Zh. Eksperim. i Teor. Fiz. 36, 204 (1959) [Soviet Phys. JETP 9, 138 (1959)].

[12]I. S. Gradshteyn and I. M. Ryzhik, Table of Integrals, Series, and Products (Academic, New York, 1965).

[13]R. Courant and D. Hilbert, Methods of Mathematical Physics, Vol. I (Interscience, New York, 1953).

Hartree-Fock Wave Functions without Symmetry and Equivalence Restrictions and the Calculation of Hyperfine-Structure Expectation Values for the Lowest ^2P States of Boron and Lithium*

Sven Larsson†

Department of Chemistry, Queen's University, Kingston, Ontario, Canada

(Received 26 March 1970)

The spin-polarized (SPHF) and unrestricted (UHF) Hartree-Fock equations are solved for the lowest ^2P states of Li and B. The orbitals are not symmetry adapted with respect to $\vec{l}^{\,2}$ in the UHF approximation for these states. The most important admixture, and the only one that has been taken into account here, is d_0 admixture into the s orbitals. The UHF determinant is not an eigenfunction of $\vec{L}^2$ and $\vec{S}^2$. Various aspects of this fact are pointed out and discussed. The admixture of d character into the orbitals will depend heavily on exchange. It will lead to substantial corrections to hyperfine-structure expectation values. The results agree well with Sternheimer's for the quadrupole terms for B and Li. For the spin dipolar term, the results agree with the first-order perturbation-theory results of Lyons et al. for Li and with the "polarization function" results of Schaefer et al. for B. Configuration interaction and second-order perturbation-theory results are also discussed in this connection.

I. INTRODUCTION

The unrestricted Hartree-Fock method (UHF) and the spin-polarized Hartree-Fock method (SPHF) are of great interest for the explanation of atomic hyperfine structure.[1] The two methods are equivalent for spherically symmetric states. For other states, SPHF is only an approximation to UHF. In this paper we shall study the UHF method for the lowest ^2P states of Li and B.

In the derivation of the SPHF equations the orbitals are assumed to be symmetry adapted, i.e., to be of the form

$$\varphi_{n\ell m_\ell m_s}(\vec{r}) = R_{n\ell m_s}(r) Y_{\ell m_\ell}(\theta, \phi) \xi_{m_s}(\xi) , \quad (1)$$

where $Y_{\ell m_\ell}$ is a spherical harmonic and ξ_{m_s} is a spin function. The radial functions R can be different in orbitals with different spins (different m_s).[2] For open-shell states the resulting SPHF orbitals will also be found to be different. This depends on the exchange interaction between the core orbitals and the outer orbitals with the same spin. As one result we will get magnetic effects,[3] for instance, hyperfine-structure effects. The Fermi contact term in hyperfine structure is defined by

$$f = 4\pi \left\langle \sum_{i=1}^{N} \delta(\vec{r}) \sigma_{z_i} \right\rangle , \qquad \sigma_{z_i} \xi_{1/2}(i) = \xi_{1/2}(i),$$

$$\sigma_{z_i} \xi_{-1/2}(i) = -\xi_{-1/2}(i) . \qquad (2)$$